HIGH RELIABILITY DIGITAL CONTROL MAGNET POWER SUPPLY SYSTEM FOR SPring-8-II

C. Kondo[†1,2], T. Masuda[1], T. Taniuchi[1], T. Fujita[1], T. Aoki[1], S. Matsubara[1], M. Tajima[1], H. Yamaguchi[1], S. Nakazawa[3], K. Fukami[1,2], T. Watanabe[1,2]
[1]Japan Synchrotron Radiation Research Institute, Hyogo, Japan
[2]RIKEN SPring-8 Center, Hyogo, Japan
[3]SPring-8 Service Co., Ltd., Hyogo, Japan

Abstract

We have developed a new magnet power supply (PS) system for the forthcoming light-source facility, SPring-8-II. Aiming for highly reliable and energy-efficient accelerator operations, various PSs have been designed to meet diverse output current and voltage requirements. Key features of this system include: (i) the integration of Silicon Carbide (SiC) switching devices in PSs for multipole magnets, aimed at enhancing power conversion efficiency; (ii) the implementation of a fully digital control system across all PSs, enabling versatile parameter configuration; and (iii) a series-connected configuration for the main PSs driving multipole magnets to minimize the frequency of PS failures. Auxiliary PSs will be provided for individual magnets where necessary to enable independent current control for betatron beating correction and other purposes. Bipolar PSs for steering magnets have been designed to provide a stable output across the entire current range, including the low-current region, by optimizing the pulse width modulation (PWM) control scheme. Additionally, we propose a cost-effective alternative utilizing shunt resistors for individual current adjustment. Furthermore, a fast PS switcher that can quickly replace a failed PS with a backup PS without beam loss is currently under development.

INTRODUCTION

The SPring-8-II upgrade project has been launched at SPring-8, with the primary goals of achieving a low emittance and establishing a green light-source facility [1, 2]. This upgrade entails the complete replacement of all magnets and the adoption of a 5-bend achromat lattice, aiming for a beam emittance of less than 100 pm·rad. To significantly reduce power consumption, permanent magnets will be employed for the bending magnets [3]. Conversely, to prioritize magnetic field tunability, electromagnets will continue to be utilized for multipole magnets (such as quadrupole, sextupole, and octupole magnets) and steering magnets [4]. Following the removal of the existing power supplies (PSs), new PSs will be custom-designed and manufactured to optimally excite these magnets. To stabilize the electron beam trajectory, these PSs aim for an output current stability on the order of 10 ppm. And, the power conversion efficiency has been designed to be as high as possible to minimize the overall energy consumption of the facility. Additionally, busbar-type PS switchers will be integrated to enable quick replacement of the PS in the event of failures, for reducing the recovery time.

Furthermore, looking toward future implementation, a fast PS switcher for a hot-swap is currently under development for improving the machine reliability of the SPring-8-II storage ring. This device is designed to rapidly substitute a failed PS with a backup one without inducing beam loss by maintaining the magnet excitation current.

This PS upgrade project originated in 2017 with the development of a high-precision, digitally controlled PS [5]. This technology has been successfully applied to magnet PSs at NanoTerasu [6] and pattern-excited magnet PSs at SACLA [7]. Based on these experiences, we optimized the final design for SPring-8-II and commenced mass production in 2025, anticipating the launch of SPring-8-II in 2029. SPring-8 is scheduled to shut down in the summer of 2027; during a period of just over a year, all existing PSs will be replaced, cables will be rewired, and comprehensive operational testing will be conducted.

This paper overviews our design of the electromagnet PS system developed for SPring-8-II and current status of the development.

POWER SUPPLY SYSTEM

The SPring-8-II storage ring comprises groups of magnets arranged in 48 cells. The overall layout is shown in Fig. 1. These 48 cells are categorized into four types: 34 normal section (NS) cells, 2 injection section (INJ) cells, 8 matching section (MS) cells, and 4 long straight

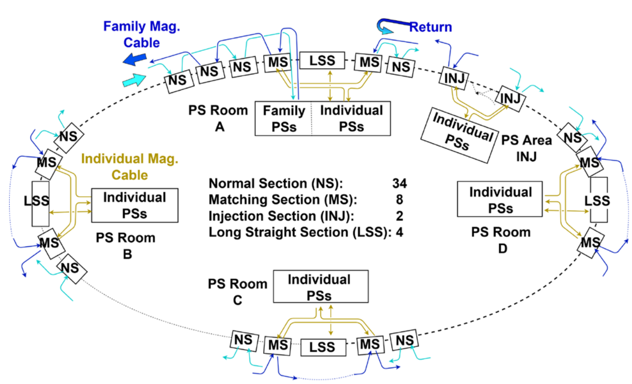

Figure 1: Overall layout of the family and individual magnets in the SPring-8-II storage ring.

†ckondo@spring8.or.jp

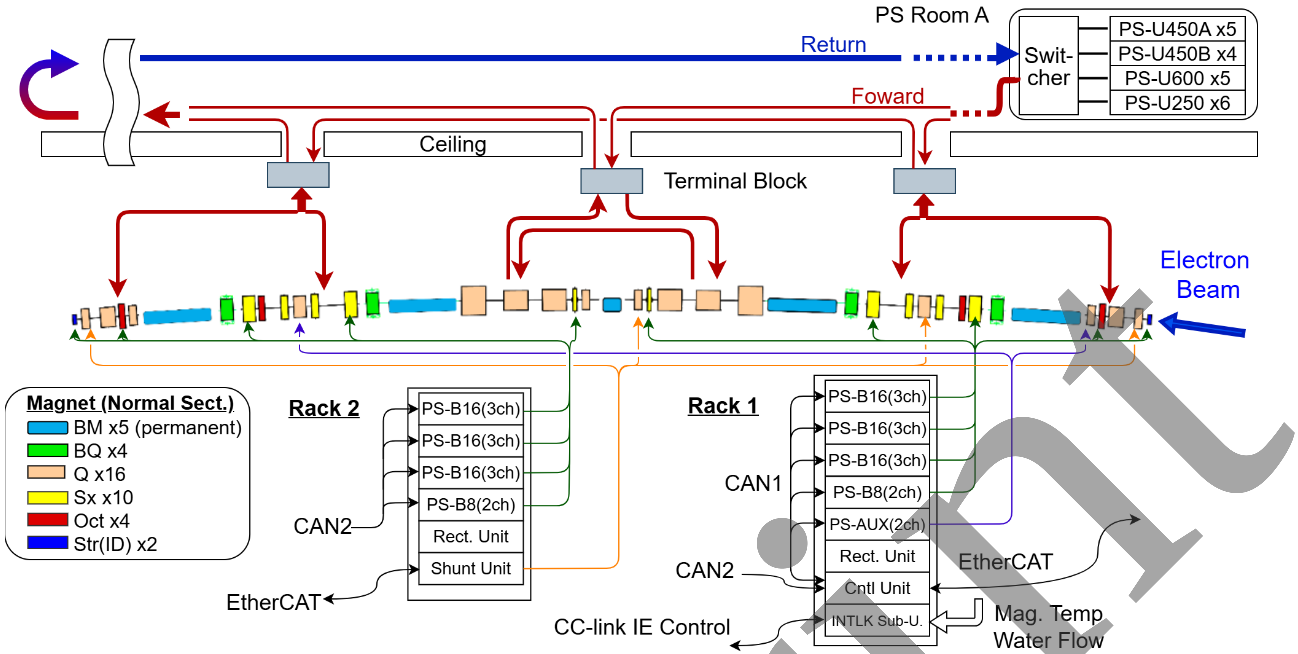

Figure 2: Schematic layout of magnets and PSs for one normal section cell.

section (LSS) cells. Most multipole magnets in the NS, INJ, and MS cells are organized into families, with 78 to 88 magnets connected in series for each family and driven by a single PS (family PS). This reduction in the total number of PSs not only reduces manufacturing costs but also minimizes the frequency of accelerator downtime caused by PS failures. All family PSs are centralized in the main PS room (PS Room A), as shown in Fig. 1. Some specific multipole magnets in the INJ, MS and LSS cells require localized excitation currents. These are driven by individual PSs, each powering one to four magnets connected in series. The individual PSs are distributed in locations nearest to the magnets (PS Rooms A–D, and PS Area INJ).

Steering and skew quadrupole fields are generated in most sextupole and octupole magnets to save space for other accelerator components. For these magnets, auxiliary coils are wound on each magnetic pole. These coils are independently excited by two or three PSs to generate the required magnetic fields. Because the total number of these magnets exceeds 1,000, their driving PSs are designed to minimize manufacturing costs by utilizing multiple outputs per unit or by sharing common rectifier and control units among several PSs.

Figure 2 illustrates the configuration of the magnets and PSs for an NS cell.

DETAILS OF PS SYSTEM

Table 1 summarizes the specifications and quantities of the family, individual and corrector PSs developed for this project. All of these PSs are designed as digitally controlled switching PSs utilizing the AMD Zynq 7000 SoC FPGA [8]. In this digital control system, operational functions such as feedback control are handled in the SoC FPGA. It can result in simplified hardware design, consisting of basic interface circuitry. Standardized FPGA firmware developed by RIKEN [5] can be easily customized for each PS through partial modifications, ensuring a straightforward development process. As a result, both development time and costs are significantly reduced. Furthermore, feedback control parameters can be easily reconfigured either via a local touch panel or through remote communication, facilitating rapid tuning. Consequently, a single PS design can be adapted to various specifications of magnets. This adaptability minimizes the number of PS models, which helps reduce mass production costs and the variety of inventories of backup PSs.

Table 1: Specifications of Magnet PSs in SPring-8-II

PS Model	Polarity	Output	Current/ Voltage	Quantity (Backup)
		Family PS		
U450A	Unipolar	1	450 A / 1000 V	5 (1)
U450B	Unipolar	1	450 A / 600 V	4 (0)
U600	Unipolar	1	600 A / 700 V	5 (1)
U250	Unipolar	1	250 A / 280 V	6 (1)
		Individual PS		
U300MS	Unipolar	1	300 A / 15 V	60 (5)
U450MS	Unipolar	1	450 A / 20 V	22 (4)
		Corrector PS		
B8	Bipolar	2	±8 A / 9 V	76 (4)
B16	Bipolar	3	±16 A / 8 V	290 (8)
AUX20	4-Quad.	2	±20 A / 10 V	53 (4)

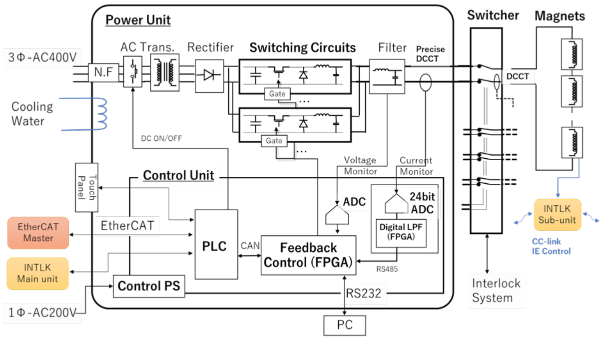

Figure 3: Schematic diagram of Family PS.

Figure 4: Photograph of test unit using SiC module.

PSs for Family Magnets

The family PSs are designed to supply an excitation current to multiple series-connected groups of magnets, requiring an output current of 250–600 A, an output voltage of 280–1000 V, and a current stability of 20 ppm or less. Figure 3 shows a block diagram of this PS. It operates as a switching PS that drives multiple switching circuits in parallel, where the number of parallel circuits can be scaled according to the rated output current. Additionally, an output-side switcher enables a quick and easy changeover to a backup PS in the event of a failure by altering busbar connections. Communication with the upper-level control system is performed via EtherCAT.

To realize a green facility, improving the power conversion efficiency of the PSs is strongly emphasized. In the case of high-power supplies such as the family PSs, employing SiC MOSFETs—which exhibit lower switching losses than conventional Insulated Gate Bipolar Transistors (IGBTs)—as switching devices can further reduce internal power loss. In addition, minimizing losses provides secondary benefits such as reducing the load on cooling equipment and enabling a more compact PS design, thereby improving maintainability.

We fabricated a prototype switching unit rated at 1.2 kV and 200 A using a 1.7 kV-rated SiC MOSFET from Mitsubishi Electric [9], and conducted switching operation tests. Figure 4 shows a photograph of the test circuit. In this setup, laminated insulated copper busbars connect the DC-link capacitor to the MOSFET, effectively restricting the

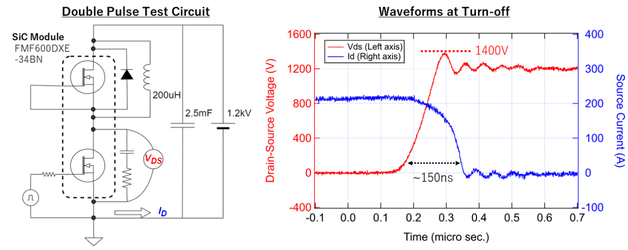

Figure 5: (Left) Circuit diagram of the double-pulse test circuit. (Right) Measured waveforms of the source-drain voltage (red) and drain current (blue) of the low-side SiC MOSFET at turn-off switching.

parasitic inductance to below 50 nH. A double-pulse test was conducted using this circuit to evaluate its switching characteristics. Figure 5 illustrates the current and voltage waveforms during turn-off. The results demonstrated a peak surge voltage of 1.4 kV, which safely fell within the module's voltage rating. Furthermore, the power loss rate in the SiC MOSFET module estimated from the measured switching waveforms and catalog values was less than 1%. Based on this result, the power losses in the switching circuit portion are expected to be reduced by more than 50% compared to conventional IGBT-based systems.

PSs for Individual Magnets

In the MS, INJ, and LSS cells, specific multipole magnets require individually adjustable excitation currents. Typically, one to four of these magnets are connected in series and driven by a single PS. These units require a high-current output rated at 300–450 A and 15–20 V. The target current stability is 20 ppm or less. Approximately 80 PS units will be deployed.

The circuit configuration is shown in Fig. 6. The circuit receives a three-phase 200 V AC input, rectifies it to DC, and performs high-frequency switching using a full-bridge inverter. The voltage is then scaled using a high-frequency transformer and rectified again. The PS enclosure is designed to be rack-mountable. Furthermore, a single control unit manages a cluster of 13–15 PSs. This control unit features a touch-panel interface for local operation and utilizes EtherCAT for communication with the upper-level control system. Inter communication between the control unit and

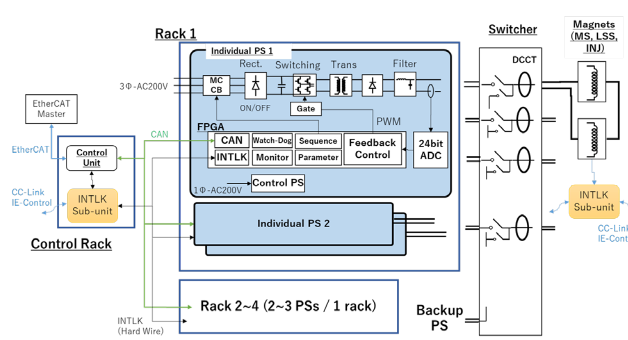

Figure 6: Schematic diagram of PSs for individual magnets.

up to 20 PS units is facilitated by a Controller Area Network (CAN) bus.

PSs for Correction Magnets

The PSs for correction magnets are utilized to excite the auxiliary coils that generate the steering and skew quadrupole magnetic fields, and to perform current corrections in the quadrupole magnets. The correction PSs are low-power units rated at 8–20 A and 8–10 V, with a maximum power capacity of 200 W. As illustrated in Fig. 7, the PS consists of multiple PS units, a single control unit, and a centralized rectifier (DC) unit. This shared-component architecture significantly reduces manufacturing costs. The rectifier unit converts 200 V AC input power into 280 V DC bus voltage, which is then distributed to the multiple PS units. Each PS unit steps down the bus voltage to 12–15 V DC voltage using a DC-DC converter, and regulates the output via a full-bridge switching circuit. A single PS unit provides two to three independent outputs.

These PSs require an output current stability of 50 ppm or less across their entire operating range. Specifically, in the low-current region near 0 A—where switching operations are prone to instability—a bipolar switching scheme is employed to ensure current stability [6].

The quadrupole correction PS (AUX PS) is designed to individually adjust the excitation current of a specific quadrupole magnet within a series-connected chain. To achieve this, the AUX PS operates in all four quadrants: it adds excitation current by increasing its output voltage relative to the load voltage supplied by the main PS (source mode), or it subtracts current by lowering its output voltage (sink mode). Detailed mechanisms of this four-quadrant operation are discussed in another paper [10]. Because the output circuit potential is tied to the load potential, the switching circuit is galvanically isolated from the ground.

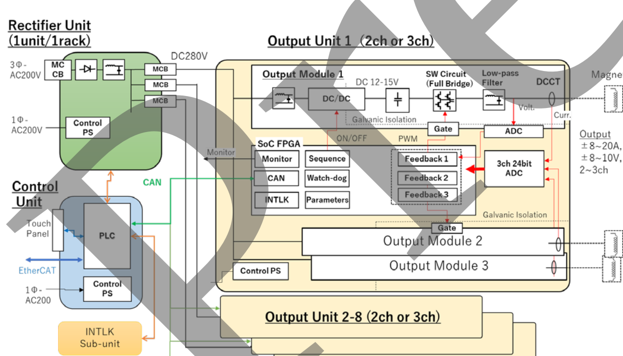

Figure 7: Schematic diagram of system of PSs for correction magnets.

Shunt Resistor System

Beam-Based Calibration (BBC) is performed to measure the offset of a beam position monitor's (BPM's) electrical center relative to the magnetic center of its adjacent quadrupole electromagnet by analyzing the beam's response to changes in quadrupole strength [11]. During this measurement, the excitation current of the quadrupole magnet nearest to the target BPM must be individually varied to discrete values. Therefore, for quadrupole magnets that are not equipped with an AUX PS, a shunt resistor circuit is employed to alter the current. In this configuration, a shunt resistor is connected in parallel with the magnet. By engaging and disengaging this resistor via a remotely controlled relay circuit, the excitation current of the magnet can be stepped by approximately 3–4%. Nearly 170 units of these shunt resistor circuits will be deployed. Because they are significantly more cost-effective than AUX PSs, this approach yields substantial cost savings.

Interlock System

Due to the complex interconnections between the magnets and PSs, the PS system incorporates a centralized interlock system designed to collectively monitor and manage equipment faults, such as insufficient cooling water flow and magnet overheating. This architecture comprises a single main unit and 54 subunits distributed across each cell and the PS rooms. These units, composed of PLC modules, are linked via the CC-Link IE Control [12]. The subunits are responsible for detecting local anomalies at the respective magnets and transmitting the diagnostic data to the main unit. Upon aggregating the fault data from the subunits, the main unit executes the required interlock logic and dispatches stop commands. These commands are transmitted directly to the family PSs or routed through the subunits to the individual and corrector PSs. Furthermore, the main unit interfaces with the facility's machine protection system to report PS fault status and receive overarching stop commands.

DEVELOPMENT OF FAST SWITCHER

Malfunctions in the magnet PSs are the primary cause of storage ring downtime. While improving the reliability of these PSs is a crucial countermeasure, further enhancing their robustness drastically increases both development time and production costs. Moreover, as the total number of deployed PSs increases, the overall frequency of downtime inevitably rises, imposing a cost-effectiveness limit on such reliability improvements. One solution to this problem is a hot-swap method already in operational use at the ESRF-EBS [13]. In the event of a PS failure, this method automatically and rapidly switches the output from the failed PS to a backup PS while maintaining the magnet excitation current, thereby preventing beam loss. Accordingly, the development of a fast PS switcher capable of hot-swapping is underway for SPring-8.

Figure 8 shows a schematic diagram of the developed fast switcher. It consists of a single control unit, a primary PS (PS1), a backup PS (PS2), and a switching unit. The switching unit is equipped with IGBT switches for the changeover, a reverse-blocking diode for each PS circuit, and a freewheeling diode connected across the positive and negative terminals. If the primary PS fails, the control unit detects the shutdown via hardwired signals and immediately turns off the primary-side IGBT. Consequently, the magnet excitation current commutates to the freewheeling diode and begins to decay gradually, at a rate determined by the resistance and inductance of the magnet and cables. During this decay period, the control unit transmits the set current and control parameters to the backup PS via RS485 communication, and subsequently, it turns on the backup-side IGBT and activates the backup PS output. The backup PS then ramps up its output current, restoring the excitation current to its pre-fault value.

A demonstration test of this fast-switching operation was conducted using an electromagnet load (2.8 mH, 10 mΩ) and two PSs (each rated at 200 A, 20 V). Figure 9 shows the output current waveforms of each PS and the excitation current waveform of the magnet during the changeover. The results confirmed that the backup PS began supplying power approximately 1.2 ms after the primary PS was stopped, and the drop in the excitation current was successfully limited to approximately 0.9%. Furthermore, it was confirmed that the excitation current could be fully restored to its nominal pre-switching value approximately 3 ms after the changeover sequence was initiated.

Going forward, we will continue the development of an even faster switcher, aiming to limit the current drop to the 0.1% level, with the goal of implementation at SPring-8-II.

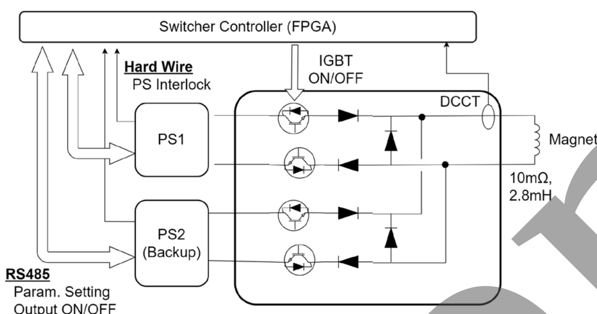

Figure 8: Schematic diagram of the fast switcher for magnet PSs.

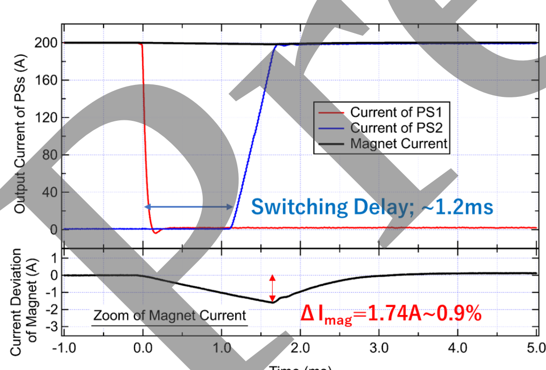

Figure 9: (Upper) Measured current waveforms of PS1 (red) and PS2(blue), and magnet(black). (Lower) Zoomed waveform of current deviation of the magnet.

CONCLUSION

For the SPring-8-II upgrade, digitally controlled electromagnet PSs featuring a high current stability of 20–50 ppm are to be developed. These PSs are classified into three categories: family, individual, and corrector PSs. For family PSs, to promote energy conservation, a switching unit using SiC MOSFETs has been adopted, enabling a significant reduction in output loss compared to conventional IGBT switching circuits. Because a large number of individual and corrector PSs are required, cost-reduction measures, such as sharing control units or rectifier units, are being pursued. Both family and individual PS systems are equipped with busbar-type switches, facilitating a quick changeover to backup units and thereby minimizing recovery time in the event of a PS failure. In future operations, the implementation of fast PS switchers capable of hot-swapping is planned to further enhance the overall reliability of the facility.

ACKNOWLEDGEMENTS

We thank K. Suda and many technical staff members at Kudo Electric Co. Ltd., for the efforts in the fabrication and testing of the fast switcher.

REFERENCES

[1] T. Watanabe and H. Tanaka, "SPring-8 Upgrade Project: Accelerator Redesigned and Restarted," *Synchrotron Radiat. News*, vol. 36, no. 1, pp. 3–6, Jan. 2023. doi:10.1080/08940886.2023.2186117

[2] H. Tanaka *et al.*, "Green upgrading of SPring-8 to produce stable, ultrabrilliant hard X-ray beams," *J. Synchrotron Radiat.*, vol. 31, no. 6, pp. 1420–1437, Oct. 2024. doi:10.1107/s1600577524008348

[3] T. Taniuchi *et al.*, "Fabrication of Permanent-Magnet-Based Longitudinal Gradient Bend for SPring-8-II", *Proc.* PASJ2025, Tokyo, Japan, August, 2025, pp.402-406

[4] K. Fukami *et al.*, "Magnet Developments and Precise Alignment Schemes for SPring-8-II", in *Proc. IPAC'19*, Melbourne, Australia, May 2019, pp. 4158-4160. doi:10.18429/JACoW-IPAC2019-THPTS024

[5] K. Fukami *et al.*, "Magnet Developments and Precise Alignment Schemes for SPring-8-II", in *Proc. IPAC'19*, Melbourne, Australia, May 2019, pp. 4158-4160. doi:10.18429/JACoW-IPAC2019-THPTS024

[6] C. Kondo *et al.*, "High precision digital control magnet power supplies", in *Proc. IPAC'23*, Venice, Italy, May 2023, pp. 3773-3775. doi:10.18429/JACoW-IPAC2023-WEPM085

[7] C. Kondo *et al.*, "Fast Current Modulation System of Q-Magnets for Multi-Energy Operation in SACLA", *Proc.* PASJ2024, Yamagata, Japan, July 31 - August 3, 2024, pp.708-712.

[8] AMD Zynq 7000 Products Selection Guide. https://docs.amd.com/v/u/en-US/zynq-7000-product-selection-guide

[9] Datasheets of SiC Power Module, https://www.mitsubishielectric.com/semiconductors/powerdevices/datasheets/sic/fmf600dxe-34bn_e.pdf

[10] H. Takebe *et al.*, "Four-Dimensional Power Supply System for SACLA Bending Magnets", *in Proc.* PASJ2011, Tsukuba, Japan, August 2011, pp.353-356.

[11] Z. Martí, G. Benedetti, U. Iriso, and A. Franchi, “Fast beam-based alignment using ac excitations,” *Phys. Rev. Accel. Beams*, vol. 23, no. 1, Jan. 2020. doi:10.1103/physrevaccelbeams.23.012802

[12] CC-Link IE Controller Network, https://www.cc-link.org/en/networktechnology/features/cclinkie/cclinkie_c.html

[13] O. Goudard and L. Jolly “An Overview of Power Supply System of the EBS”, Accelerator Reliability Workshop (ARW) 2022, unpublished. doi:10.13140/RG.2.2.10719.53929